PHYSICAL REVIEW C
NUCLEAR PHYSICS

THIRD SERIES, VOLUME 56, NUMBER 6 DECEMBER 1997

RAPID COMMUNICATIONS

The Rapid Communications section is intended for the accelerated publication of important new results. Manuscripts submitted to this section are given priority in handling in the editorial office and in production. A Rapid Communication in **Physical Review C** *may be no longer than five printed pages and must be accompanied by an abstract. Page proofs are sent to authors.*

Influence of the ground state spin of target nuclei on the anomalous behavior of fission fragment anisotropies

J. P. Lestone, A. A. Sonzogni, M. P. Kelly, and R. Vandenbosch
Nuclear Physics Laboratory 354290, University of Washington, Seattle, Washington 98195
(Received 23 June 1997)

The angular distributions of fission fragments have been measured over a range of near- and sub-barrier energies for reactions involving ^{12}C projectiles on ^{235,236,238}U targets. For the reactions involving the zero spin targets, the discrepancies between the experimental fission anisotropies and the transition state model increase dramatically as the beam energy decreases through the region of the fusion barriers. However, the $^{12}\mathrm{C}+(I=7/2)^{235}\mathrm{U}$ fission anisotropies exhibit a much less dramatic departure from the transition state model. [S0556-2813(97)50312-8]

PACS number(s): 25.70.Jj

An important part of nuclear physics is understanding the time scales associated with equilibrating various degrees of freedom. In this paper we focus on the angular momentum degrees of freedom and specifically on the tilting mode associated with the orientation of the symmetry axis of a deformed nucleus relative to the total angular momentum. The projection of the total angular momentum, $J\hbar$, onto the symmetry axis, $K\hbar$, can be probed by measuring the angular distribution of fission fragments. At bombarding energies sufficiently above the fusion barrier the transition state model [1] is quite successful in accounting for measured angular distributions. In this model the distribution of K states for fissioning systems is determined by the moment of inertias at the fission saddle point and the nuclear temperature, T. In recent years there has been much interest in the failure of the transition state model of fission fragment angular distributions in sub-barrier heavy-ion reactions involving actinide targets. Two of the more popular models that attempt to explain the anomalously high fission fragment anisotropies [$A=W(180°)/W(90°)$] in near- and sub-barrier reactions are the preequilibrium K-states model [2–5] and the orientation-dependent quasifission model [6]. The main predictions of the preequilibrium K-states model are that for reactions with entrance channel mass asymmetries $\alpha=(A_T-A_P)/(A_T+A_P)$ larger than the Businaro-Gallone (BG) critical mass asymmetry of $\alpha_{cr}\sim0.9$ [7] the standard transition state model (TSM) of nuclear fission [1] should adequately reproduce observed fission anisotropies, and that for heavy systems formed in reactions with $\alpha<\alpha_{cr}$ the observed fission anisotropies should be anomalously high at low beam energies due to an increase in the K-states equilibration time with decreasing angular momentum. In the orientation-dependent quasifission model [6] it is assumed that if the point where the projectile fuses with a prolate deformed actinide target has an angle to the target's symmetry axis ϕ larger than some critical value ϕ_{cr}, then standard fusion occurs and the angular distribution of the fission fragments is given by the TSM. When $\phi<\phi_{cr}$, a dinucleus is assumed to be formed with a deformation greater than the saddle point of the corresponding system and this system then fissions quickly (quasifission) with an anisotropy greater than the value predicted by the TSM.

Another possible explanation of the anomalously high fission fragment anisotropies in near- and sub-barrier reactions has been proposed [8] but has received little attention. We shall refer to this model as the entrance channel dependent (ECD) K-states model. The main ingredients of this model are that immediately following fusion the system has the K-state distribution of the entrance channel and that this initial distribution is broadened with time due to a coupling between the intrinsic and collective rotational degrees of freedom. For reactions involving zero spin projectiles and targets, the distribution of spins about the target's symmetry axis K, for a total spin J, is given by

$$P(K)dK=\frac{2}{\pi J\ \sin\ \phi}\frac{dK}{\sqrt{1-(K/[J\ \sin\ \phi])^2}}, \qquad (1)$$

where ϕ is the angle from the point of interaction to the symmetry axis of the target and $0\leqslant K<J\ \sin\ \phi$. At well-above-barrier energies an integral over all possible interaction points yields a uniform K-state distribution for each J. At sub-barrier energies, where the projectiles interact preferentially with the tips of prolate target nuclei, the entrance channel K-state distributions for each J are strongly peaked at $K=0$ for reactions involving spin zero targets.

Although the ECD K-states model contains a K-states equilibration time as in the pre-equilibrium K-states model [4,5], this is not the sole reason for the anomalous behavior of fission anisotropies at near- and sub-barrier energies. In the ECD K-states model an equally important role is played by the beam energy dependence of the entrance channel K-state distributions. At above-barrier energies the entrance channel K-state distributions for each J are fairly uniformly populated and thus K-state equilibration processes have little influence on the K-state distributions of the fissioning systems. At sub-barrier energies where the entrance channel K-state distributions are strongly peaked at $K=0$, the K-state distribution of fissioning systems is influenced by the relative sizes of the K-states equilibration time τ_{eq} and the fission time t_f. If $t_f\lesssim\tau_{\mathrm{eq}}$ then the ECD K-states model predicts a dramatic increase in the observed fission fragment anisotropy, relative to the transition state model, as the beam energy drops through the region of the fusion barriers.

Vorkapić and Ivanišević [8] have shown that the ECD K-states model can reproduce anomalous fission fragment angular distributions observed in the $^{12}C+^{236}U$ and $^{16}O+^{232}Th$ reactions. It should be noted that even though these two reactions have entrance channel mass asymmetries on either side of the BG critical asymmetry, the ECD K-states model is capable of reproducing the measured fission fragment anisotropies for both reactions without any reference to the entrance channel mass asymmetry relative to the BG critical value. This suggests that, contrary to the conclusions drawn by others [2–5], the BG critical mass asymmetry plays little role in determining fission fragment anisotropies.

In sub-barrier reactions on actinide targets with nonzero ground state spin I, the entrance channel K-state distributions are not peaked at $K=0$ but at $K=\pm I$. Due to the low angular momentum involved in sub-barrier reactions, this dependence of the entrance channel K-state distributions on I may lead to an influence of the ground state spin of target nuclei on the anomalous behavior of fission anisotropies. The aim of the present study was to test for this possibility.

We have studied the cross sections, angular distributions, and folding angle distributions for $^{12}C+^{235,236,238}U$ fission fragments at near- and sub-barrier energies using pulsed heavy-ion beams from the University of Washington tandem plus superconducting linear accelerator [9]. The beam pulses had a width of <1 ns and were separated in time by 80 ns. The ^{12}C beam currents varied from 150 nA to 500 nA. The ^{238}U target was a 250-μg/cm^2-thick layer of UF_4 evaporated onto a 20 μg/cm^2 C foil. For the shorter lived $^{235,236}U$ isotopes, the targets consisted of 70 ± 20 μg/cm^2 and 25 ± 5 μg/cm^2 of uranium-oxides electroplated onto ~250 μg/cm^2 Ni foils, respectively. Singles fission fragment angular distributions were measured using two Si surface barrier telescopes. These telescopes were ~15 cm from the target and remotely rotated about the target position between beam runs enabling us to cover the angular range from $\theta_{\mathrm{lab}}=82°$ to 170°. Fission fragments were clearly identified at all angles and beam energies using energy-loss, energy, and time-of-flight information. The fission fragment angular distributions were determined by normalizing the fission fragment yields in one of the telescopes to the fission yield of the other telescope at a fixed position and by normalizing the yields in both telescopes at various angles to the integrated beam current and the intensity of incident ions elastically scattered from the uranium nuclei into a Si surface barrier detector located at an angle between 17° and 33°. The angle of this Si detector was occasionally changed to keep the elastic scattering rate at a reasonable level. The fission anisotropies obtained using these three normalization methods were found to be in good agreement within experimental errors. Figure 1 shows our $E_{\mathrm{lab}}=65$ MeV $^{12}C+^{235}U$ and $^{12}C+^{238}U$ fission fragment angular distributions. Our measured singles $^{12}C+U$ fission fragment anisotropies are shown in Fig. 2 along with previous measurements [10,11].

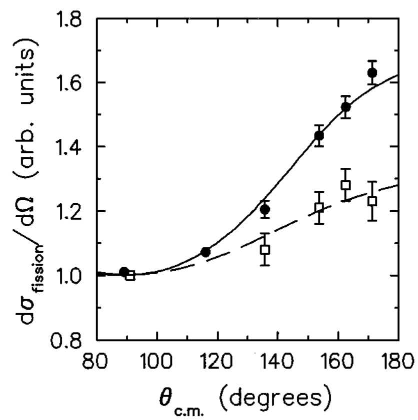

FIG. 1. $E_{\mathrm{lab}}=65$ MeV $^{12}C+^{235}U$ (open squares) and $^{12}C+^{238}U$ (solid circles) fission fragment angular distributions. The curves show transition state model calculations with the variance of the K-state distribution varied as a free parameter to obtain the best fit to the individual angular distributions.

The fission cross sections were determined by normalizing to the intensity of incident ions elastically scattered from the uranium nuclei into the forward located Si surface barrier detector. The relative solid angles of the detectors were determined using an alpha source placed at the target position. The quality of the ^{238}U target was such that the accuracy of fission cross sections obtained using this target was defined by the uncertainties in the relative solid angles of the detectors and by counting statistics. However, for the $^{235,236}U$ targets, the elastic scattering from the actinides could not be cleanly separated from the elastic scattering from the backing materials. This led to uncertainties in the absolute fission cross sections obtained using these targets of $\sim20\%$. This

RAPID COMMUNICATIONS

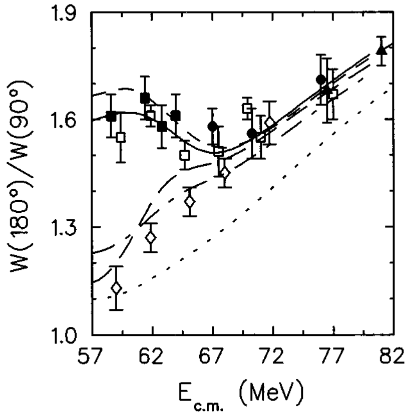

FIG. 2. Measured C+U fission fragment anisotropies as a function of $E_{c.m.}$. $^{12}C+^{235}U$ open diamonds; $^{12}C+^{236}U$ filled circles, filled squares [10], and filled triangles [11]; and $^{12}C+^{238}U$ open squares. The curves are model calculations (see text).

does not, however, influence the accuracy of our measured relative differential fission cross sections.

The present C+U fission cross sections and the $^{12}C+^{236}U$ measurements of [10,11] are shown in Fig. 3. The solid line is a calculation of the $^{12}C+^{236}U$ fusion cross sections obtained using a code which takes into account the effects of statically deformed potentials. Due to the high fissility of the compound nuclei involved, the fission and fusion cross sections are essentially the same quantity. Deformed nuclear and Coulomb potentials were calculated based on the optical model potentials of [12] with a static quadrupole deformation of the U targets $\beta_2=0.28$ [13]. To obtain the excellent fit to the data shown in Fig. 3, the nuclear radii of [12] were scaled by 1.013. The dashed line shows the calculated cross sections assuming a spherical target.

To check for the presence of any significant transfer-fission yield in our $^{12}C+^{235,236,238}U$ reactions we have measured the folding angle distribution for events with $\theta_{c.m.}\sim 90°$. This was done by observing fission fragments in one of our Si telescopes at $\theta_{lab}=82°$ in coincidence with the complementary fragment in a 6 cm×4 cm Si strip detector

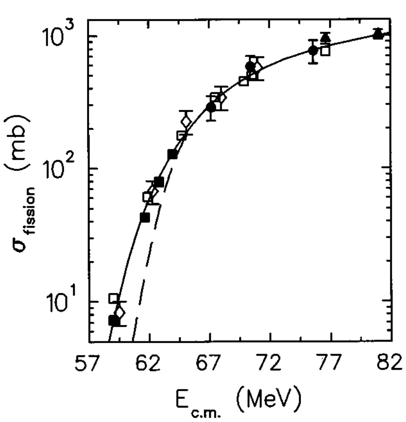

FIG. 3. C+U fission cross sections $\sigma_{fission}$ as a function of $E_{c.m.}$. $^{12}C+^{235}U$ open diamonds; $^{12}C+^{236}U$ filled circles, filled squares [10], and filled triangles [11]; and $^{12}C+^{238}U$ open squares. The curves are model calculations (see text).

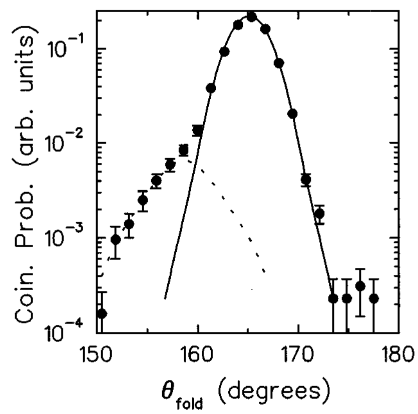

FIG. 4. Our $E_{lab}=65$ MeV $^{12}C+^{238}U$ fission fragment folding angle distribution. The solid and dashed lines show the fusion-fission and transfer-fission components, respectively, determined assuming that both these components have a symmetric folding angle distribution.

~ 35 cm from the target at angles close to $\theta_{lab}=-82°$ on the other side of the beam axis. By changing the angle of the strip detector the full horizontal range of the fragment-fragment coincidence was covered. Our folding angle distributions are peaked within $\lesssim 0.6°$ of the angles expected for symmetric fission following complete fusion. Our folding angle distributions have a FWHM of $\sim 5°$ and are symmetric down to a factor of 10 below the peak height. Below this point an asymmetry in our folding angle distributions is seen. This asymmetric component does not change significantly as one drops the beam energy through the region of the fusion barriers. If we assume that the asymmetry is due solely to transfer fission then we estimate that transfer fission is responsible for only $\sim 5\%$ of the total fission yield. We thus conclude that in C+U reactions the fission yield is dominated by fission events following complete fusion of the projectile. This observation is consistent with the findings of [4,14–17] for a range of reactions involving *B* and *C* projectiles on actinide targets. Figure 4 shows our $E_{lab}=65$ MeV $^{12}C+^{238}U$ folding angle distribution. The expected folding angle for symmetric fission following complete fusion is $\theta_{fold}\sim 165.3°$, in agreement with our measured distribution. The asymmetry at the lower folding angles is likely due to fission following the α and 2α transfer channels. These are the only two likely transfer channels with optimum *Q* values in excess of the fission barriers of the relevant actinide nuclei. The expected mean folding angle for fission following these two transfer channels is 155.5° and 160.3°, respectively. The solid and dashed lines in Fig. 4 show the fusion-fission and transfer-fission components, respectively, determined assuming that both these components have a symmetric folding angle distribution. Based on our present folding angle distributions and the work of [4,14–17], we believe that the transfer-fission corrections to our singles anisotropy data shown in Fig. 2 will be no larger than our quoted experimental errors.

In view of the excellent agreement between the measured and the calculated cross sections shown in Fig. 3, we used our fusion cross section code to estimate the total spin distribution $\sigma_{fus}(J)$, the distribution of projectile-target interac-

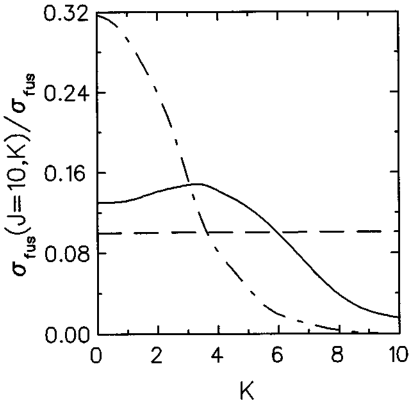

FIG. 5. The dashed curve shows the $J=10$, K-state distribution for the $^{12}C+^{235,236}U$ reactions at $E_{c.m.}=75$ MeV. The solid and dash-dotted lines show the $J=10$ K-state distributions for the $^{12}C+^{235}U$ and $^{12}C+^{236}U$ reactions at $E_{c.m.}=55$ MeV, respectively.

tion points $d\sigma_{fus}(J,\phi)/d\phi$, and the entrance channel K-state distributions $d\sigma_{fus}(J,\phi,K)/d\phi$. The dashed and dash-dotted lines in Fig. 5 show calculated $J=10$ K-state distributions,

$$\sigma_{fus}(J=10,K)=\int\frac{d\sigma_{fus}(J=10,\phi,K)}{d\phi}d\phi, \tag{2}$$

for $^{12}C+^{236}U$ at $E_{c.m.}=75$ and 55 MeV, respectively. The fusion barrier for C+U reactions is ~ 65 MeV. The K-state distributions are fairly uniform at well-above-barrier energies while at sub-barrier energies the K-state distributions for reactions involving spin zero targets become strongly peaked at $K=0$. This is because the projectile cannot bring in much angular momentum about the target's symmetry axis if it is interacting with one of the tips of the prolate target. The solid line in Fig. 5 is the $J=10$ K-state distribution for $^{12}C+^{235}U$ at $E_{c.m.}=55$ MeV. At sub-barrier energies the K-state distributions for $^{12}C+^{235}U$ peak at $\pm 7/2$ due to the projection of the ground state spin of the target along the symmetry axis.

The dotted line in Fig. 2 shows a transition state model calculation for the $^{12}C+^{236}U$ reaction. Presaddle neutron emission corrections were made assuming that the presaddle neutron multiplicities, as a function of initial excitation energy, are half the measured prescission multiplicities of [18]. Varying the presaddle multiplicities from 0 to the prescission values makes only minor changes to the calculations shown. In the calculation of the nuclear temperature T a level density parameter $a=A/8.5$ MeV^{-1} was used and 8 MeV was removed from the initial excitation energy for each presaddle neutron evaporated. The experimental $^{12}C+^{236,238}U$ anisotropies are clearly anomalously high at sub-barrier energies while the corresponding $^{12}C+(I=7/2)^{235}U$ results are qualitatively different.

Assuming, for the moment, that the spin about the beam axis is $M=0$, the angular distribution of fission fragments relative to the beam direction θ can be written as [19]

$$W(\theta)=\sum_{J,K}\frac{P(J,K)}{4}(2J+1)(|d^J_{M=0,K}|^2+|d^J_{M=0,-K}|^2), \tag{3}$$

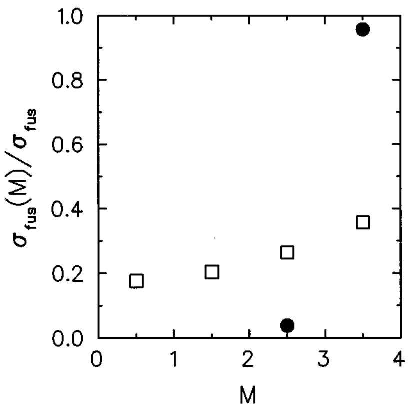

FIG. 6. $^{12}C+^{235}U$ M-state distributions at $E_{c.m.}=55$ MeV (solid circles) and $E_{c.m.}=75$ MeV (open squares).

where $P(J,K)$ is the probability of a fissioning system having the quantum numbers J and K. In the ECD K-states model $P(J,K)$ is given by

$$P(J,K)\propto\int\sigma_{fus}(J,K')\exp[-(K-K')^2/(2\sigma_K^2)]dK' \times\exp[-(K\hbar)^2/(2\mathfrak{I}_{eff}T)]. \tag{4}$$

K' represents the initial K states populated by the entrance channel. $P(J,K)$ is the initial K-state distribution for each J convoluted by a Gaussian with standard deviation σ_K and multiplied by the TSM filtering effect of the fission saddle point. After reviewing the theoretical work of Døssing and Randrup [20] on the equilibration of K states, we modelled the equilibration of the entrance channel K-state distributions using

$$\sigma_K=qJ\sqrt{Tt}, \tag{5}$$

where t is the time and q is a constant to be determined from the experimental data. To determine σ_K at the time of fission we used the mean Bohr-Wheeler fission time

$$\tau_f=\frac{2\pi}{\omega_{eq}}\exp\left(\frac{B(J)}{T}\right), \tag{6}$$

where $B(J)$ are finite-range-corrected fission barriers [21]. For simplicity ω_{eq} was set equal to 10^{+21} s^{-1}.

The short-dashed and solid lines in Fig. 2 show the $^{12}C+^{236}U$ and ^{238}U (both $I=0$) fission fragment anisotropies, respectively, calculated using the above procedure with $q=0.074$ (MeV$\times 10^{-21}$ s)$^{-1/2}$. The long-dashed curve shows the same calculation but for the $^{12}C+^{235}U$ reaction. The agreement between the model calculations and our measured $^{12}C+^{235}U$ anisotropies can be improved at near-barrier energies if the $M\neq 0$ states produced by the 7/2 spin of the ^{235}U target nuclei are taken into account. We have made a simple semiclassical estimate of the M-state distributions using the projection of the target spin along the beam axis at the time of fusion. Figure 6 shows M-state distributions

$$\sigma_{fus}(M)=\sum_{J,K}\int\frac{d\sigma_{fus}(J,\phi,K,M)}{d\phi}d\phi \tag{7}$$

for $^{12}C+^{235}U$ at $E_{c.m.}=55$ and 75 MeV. At well-above-barrier energies all interaction angles ϕ contribute significantly to the fusion process and thus the M-state distributions are fairly uniformly populated from $-I$ to $+I$. At sub-barrier energies where the projectiles interact predominately with the tips of the prolate target nuclei whose symmetry axes are aligned in the beam direction, the fusion M-state distributions are strongly peaked at $\pm I$. Incorporating the effects of the $M\neq 0$ states into Eq. (3) by including a sum over all possible M, leads to the $^{12}C+^{235}U$ calculation shown by the dash-dotted curve in Fig. 2. These simple but quantitive model calculations reproduce the main features of the $^{12}C+^{235,236,238}U$ data.

Our measured C+U fission anisotropies show anomalous behavior relative to the transition state model despite having an entrance channel mass asymmetry larger than the Businaro-Gallone critical value. This anomalous behavior has a dependence on the ground state spin of the U isotopes in agreement with the ECD K-states model. An estimate of the K-states equilibration time can be obtained by setting Eq. (5) equal to $J/2$ with $q=0.074$ (MeV$\times 10^{-21}$ s)$^{-1/2}$ and the mean fission time as in Eq. (6). This gives a K-states equilibration time of $\tau_K \sim 5/T$ MeV$\times 10^{-20}$ s. From our present analysis we conclude that the anomalous behavior of fission fragment anisotropies at sub-barrier energies is not associated with either the BG critical mass asymmetry or the occurrence of quasifission but is due to a memory of low K states populated during the fusion of projectiles with the tips of prolate targets.

This work was supported in part by the U.S. Department of Energy.

[1] R. Vandenbosch and J. R. Huizenga, *Nuclear Fission* (Academic Press, New York 1973).
[2] V. S. Ramamurthy and S. S. Kapoor, International Conference on Nuclear Physics, Harrogate, United Kingdom, 1986, IOP Conference Proceedings No. 86 (Institute of Physics, Bristol, 1986), Vol. 1, p. 292.
[3] V. S. Ramamurthy *et al.*, Phys. Rev. Lett. **65**, 25 (1990).
[4] Z. Liu, H. Zhang, J. Xu, Y. Qiao, X. Qian, and C. Lin, Phys. Rev. C **54**, 761 (1996).
[5] Z. Liu, H. Zhang, J. Xu, Y. Qiao, X. Qian, and C. Lin, Phys. Lett. B **353**, 173 (1995).
[6] D. J. Hinde, M. Dasgupta, J. R. Leigh, J. P. Lestone, J. C. Mein, C. R. Morton, J. O. Newton, and H. Timmers, Phys. Rev. Lett. **74**, 1295 (1995).
[7] U. L. Businaro and S. Gallone, Nuovo Cimento **5**, 315 (1957); K. T. R. Davies and A. J. Sierk, Phys. Rev. C **31**, 915 (1985).
[8] D. Vorkapić and B. Ivanišević, Phys. Rev. C **52**, 1980 (1995).
[9] D. W. Storm, J. F. Amsbaugh, D. T. Corcoran, G. C. Harper, M. A. Howe, R. E. Stowell, W. G. Weitkamp, T. D. Van Wechel, and D. I. Will, Nucl. Instrum. Methods Phys. Res. A **287**, 247 (1990).
[10] T. Murakami, C. C. Sahm, R. Vandenbosch, D. D. Leach, A. Ray, and M. J. Murphy, Phys. Rev. C **34**, 1353 (1986).
[11] R. Vandenbosch, J. D. Bierman, J. P. Lestone, J. F. Liang, D. J. Prindle, A. A. Sonzogni, S. Kailas, D. M. Nadkarni, and S. S. Kapoor, Phys. Rev. C **54**, R977 (1996).
[12] M. Lozano and G. Madurga, Nucl. Phys. **A334**, 349 (1980).
[13] S. Raman, C. H. Malarkey, W. T. Milner, C. W. Nestor, Jr., and P. H. Stelson, At. Data Nucl. Data Tables **36**, 1 (1987).
[14] J. C. Mein, Dept. of Nucl. Phys., ANU, Annual Report 1995, ANU-P/1196, p. 56.
[15] J. P. Lestone, A. A. Sonzogni, M. P. Kelly, and D. Prindle, Phys. Rev. C **55**, R16 (1997).
[16] J. C. Mein, D. J. Hinde, M. Dasgupta, J. R. Leigh, J. O. Newton, and H. Timmers, Phys. Rev. C **55**, R995 (1997).
[17] J. P. Lestone, A. A. Sonzogni, M. P. Kelly, and R. Vandenbosch, Phys. Rev. Lett. (to be published).
[18] A. Saxena, A. Chatterjee, R. K. Choudhury, S. S. Kapoor, and D. M. Nadkarni, Phys. Rev. C **49**, 932 (1994).
[19] B. B. Back and S. Bjørnholm, Nucl. Phys. **A302**, 343 (1978).
[20] T. Døssing and J. Randrup, Nucl. Phys. **A433**, 215 (1985).
[21] A. J. Sierk, Phys. Rev. C **33**, 2039 (1986).